ACS OMEGA

Open Access

http://pubs.acs.org/journal/acsodf

Article

Rh(II)-Catalyzed Si−H Insertion with Nosyl-hydrazone-Protected Aryl Donor Diazo Compounds

Anthony Abshire, Bukola Ogunyemi, and Ampofo Darko*

Cite This: *ACS Omega* 2023, 8, 38005−38012

Read Online

ACCESS | Metrics & More | Article Recommendations | Supporting Information

ABSTRACT: Dirhodium(II,II) paddlewheel catalysts were evaluated in silyl-hydrogen insertion reactions of aryl diazo compounds generated from *o*-nosyl hydrazones. The high reactivity of aryl diazo compounds necessitates their in situ generation from sulfonyl-protected hydrazones. Herein, we describe our efforts to evaluate this transformation utilizing Rh(II) catalysts, including those with tethered, axially coordinating ligands. The heteroleptic catalyst, $Rh_2(OAc)_3$(2-OX), provided the highest yield of silanes when dioxane was the solvent.

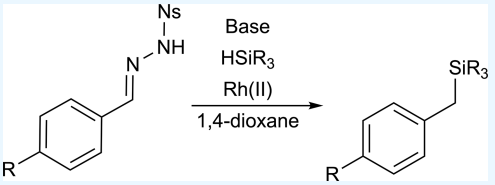

INTRODUCTION

The carbene transfer reaction has greatly increased the synthetic chemist's ability to complete various transformations such as cyclization reactions,[1] X−H functionalization (X = C, N, B, O, S, Si, Ge, Sn, and P),[2] and ylide transformations.[3] One of the most broadly used carbene precursors is the diazo compound, which can be divided into five separate classes based on the donor and acceptor combination of flanking substituents. Donor-type diazo compounds, in contrast to donor−acceptor and acceptor-type diazo compounds, have had limited impact in carbene transfer reactions due to their inherent instability.[4] As a result, they must be transported and stored in dilute solutions at low temperatures prior to their usage.

Due to the unstable nature of donor-type diazos, alternative precursors have been developed.[4a] Nondiazo precursors that produce donor-type carbenes include hydrazones, allenes, cyclopropenes, cycloheptatrienes, propargyl esters and ethers, enynes, and enynones. Hydrazones are one of the most popular precursors because of their controlled decomposition to diazo, thereby limiting the buildup of reactive species in solution. Typical conditions of hydrazone decomposition require moderate base and polar aprotic solvent at elevated temperatures.[5]

While donor-type diazos are highly reactive, carbenes derived from them are very stable, and this inverse relationship is common between metal carbene and diazos, described as umpolung reactivity, in which the donor-type diazo compound is highly nucleophilic while the donor-type metal carbene is electrophilic. As a demonstration of their stability, donor−donor carbenes are the only type of carbenes that have been successfully isolated. A *para*-methoxy substituted diaryl carbene was isolated and characterized by Fürstner and co-workers,[6] which was the first report of a crystal structure of any dirhodium carbene complex. Their umpolung reactivity, although, means that homocoupling, or formal dimerization, of diazo compounds is a competing reaction that must be overcome.

Although the emergence of donor diazo carbene transfer reactions is relatively new in comparison to other types, they have been used in carbene transfer reactions, such as Si−H insertion reactions. A disclosure from Liu et al. in 2017 reported the insertion of donor-type carbenes into Si−H, Ge−H, and Sn−H bonds.[7] However, these transformations were performed at a high 30% catalyst loading with silver(I) triflate. The silver(I) triflate catalyst proved tolerant of many functional groups while smoothly inserting into the group 12 atom hydrogen bond in high yield, but aliphatic hydrazones failed to convert into the desired silane by this method. The following year, Wang et al. reported Si−H, Ge−H, and Sn−H insertions utilizing an iron porphyrin catalyst.[8] This was achieved with 2 mol % catalyst loading and showcased insertion into primary, secondary, and tertiary Si−H bonds at high temperatures. In 2018, Liu et al. published a Pd(0)-catalyzed Si−H insertion from N-tosylhydrazones and demonstrated a broad scope with broad functional group tolerance but also required high temperatures to proceed.[9]

Diazo-mediated insertion reactions into Si−H reactions have a long history dating back to the seminal report of diazoalkane insertion into organosilanes in 1963.[10] Doyle was the first to report Rh(II) catalyzed Si−H insertion,[11] and others[12] such as Landais,[13] Hashimoto,[14] and Ball[15] have followed with advancements in Rh(II)-catalyzed Si−H insertion, often using donor/acceptor diazo compounds as carbene precursors and obtaining products with good to excellent diastereo- and

Received: May 19, 2023
Accepted: September 7, 2023
Published: October 6, 2023

enantioselectivity. Although Rh(II) paddlewheel complexes are used quite prevalently for insertion reactions, few reports of Si−H insertion with donor-type diazo compounds using Rh(II) paddlewheel complexes have been reported. Recently, donor/donor diazo compounds have been reported for chiral Si−H insertion reactions[16] using a chiral homoleptic rhodium catalyst in tandem with silicon-stereogenic silanes to promote selectivity (Figure 1a),[16a] but reports of good performance of

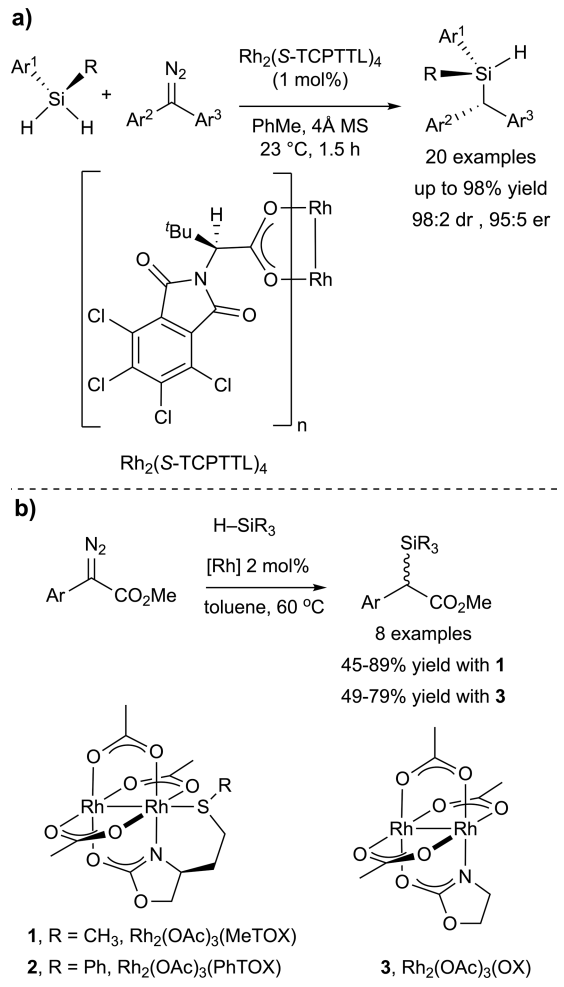

Figure 1. (a) Enantioselective Rh(II)-catalyzed Si−H insertion with diaryl carbenes and (b) Si−H insertion catalyzed by dirhodium complexes with tethered axially coordinated thioether ligands.

Rh(II) catalysts with donor-type carbenes are rare. In our previous work, we described Rh(II) paddlewheel complexes with tethered, axially coordinated ligands (TACLs) as efficient Si−H insertion catalysts with donor/acceptor diazo compounds (Figure 1b).[17] In our studies, we noticed higher yields for electron rich aryl diazo acetates and were intrigued by the possibility of expanding Si−H insertion using Rh(II) TACLs complexes to donor-type carbenes. In addition, the ability of Rh(II) catalysts to perform reactions at low catalyst loadings[18] and mild reaction conditions[14] prompted us to further study their utility in this reaction. The benzyl silanes that result from the insertion reaction are useful as chiral auxiliaries[19] and as intermediates in the synthesis of biologically active compounds,[20] so their mild and efficient synthesis is important.

RESULTS AND DISCUSSION

We began our reaction optimization by screening solvents with the nosyl-protected aryl hydrazone (**4a**),[7] 1.5 equiv of sodium hydride, 5 mol % of our previously developed catalyst, $Rh_2(OAc)_3$(MeTOX) (**1**), and 5 equiv of dimethylphenylsilane at 25 °C for 24 h. The thioether tethered catalyst converted the hydrazone to the desired silane in only 12% yield in dichloromethane (Table 1, entry 1). The use of

Table 1. Reaction Optimization[a]

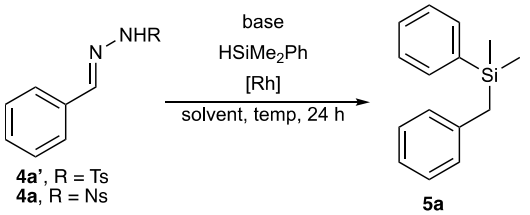

entry	R	[Rh] cat	base	solvent	temp (°C)	yield (%)[b]
1	Ns	**1**	NaH	CH_2Cl_2	25	12
2	Ns	**1**	NaH	ACN	25	20
3	Ns	**1**	NaH	THF	25	10
4	Ns	**1**	NaH	DCE	25	7
5	Ns	**1**	NaH	dioxane	25	60
6	Ns	**1**	^{t}BuOK	dioxane	25	56
7	Ns	**1**	Cs_2CO_3	dioxane	25	57
8	Ns	**1**	NaHMDS	dioxane	25	71
9	Ns	**1**	NaHMDS	dioxane	40	60
10	Ns	**1**	NaHMDS	dioxane	80	50
11	Ns	**2**	NaHMDS	dioxane	25	67
12	Ns	$Rh_2(OAc)_4$	NaHMDS	dioxane	25	74
13	Ns	**3**	NaHMDS	dioxane	25	78
14	Ts	**3**	NaHMDS	dioxane	25	15
14[c]	Ns	$Rh_2(OAc)_4$	NaHMDS	dioxane	25	11
15[c]	Ns	**3**	NaHMDS	dioxane	25	11
16[c]	Ns	**1**	NaHMDS	dioxane	25	29

[a]Reaction conditions: **4a** or **4a'** (0.065 mmol), base (0.098 mmol), dimethylphenylsilane (0.33 mmol), Rh cat (5.0 mol %) in solvent (1.25 mL) for 24 h. [b]Yields determined by ^{1}H NMR with reference to mesitylene as an internal standard. [c]Performed with 2.0 mol % catalyst.

acetonitrile as the reaction solvent increased the yield to 20% yield, while a 10% yield was obtained in tetrahydrofuran (Table 1, entries 2 and 3). We then evaluated 1,2-dichloroethane as the reaction solvent and found that it was also a poor solvent to facilitate this transformation (7% yield, Table 1, entry 4). Switching to 1,4-dioxane, however, resulted in a vast increase in yield to 60% (Table 1, entry 5). We then turned our attention to screening other bases. The use of potassium *tert*-butoxide slightly decreased the yield to 56% compared to sodium hydride (Table 1, entry 6). Cesium carbonate produced results similar to those of potassium *tert*-butoxide, producing 57% yield of the desired product (Table 1, entry 7). Sodium hexamethyldisilazane (NaHMDS) facilitated the degradation of the hydrazone starting material to the reactive diazo intermediate best, and the yield of the desired product was further increased to 71% (Table 1, entry 8). Increasing the reaction temperature did not have a positive effect on the yields of the insertion reaction. When the reaction was performed at 40 °C, the yield decreased by 11% (60% yield; Table 1, entry 9). A further 10% reduction of yield was

https://doi.org/10.1021/acsomega.3c03519
ACS Omega 2023, 8, 38005−38012

experienced when the temperature was elevated to 80 °C (50% yield, Table 1, entry 10). Rh(II) paddlewheel complexes can be unstable in alkaline conditions,[21] so it is possible that higher temperatures promoted degradation of the Rh(II) catalyst, thereby reducing yields. Other Rh(II) catalysts with and without TACLs were also tested. Changing the substituent on the thioether to phenyl by using $Rh_2(OAc)_3$(PhTOX) (**2**) slightly reduced the yield by 4% (67% yield, Table 1, entry 11). The benchmark Rh(II) catalyst $Rh_2(OAc)_4$, however, improved the yield to 74% (Table 1, entry 12) and the heteroleptic complex $Rh_2(OAc)_3$(2-OX) (**3**) further increased the yield to 78% (Table 1, entry 13). When *N*-tosyl hydrazone **4a**' was used with complex **3**, the product was obtained in only 15% yield. This is likely due to the relatively difficult decomposition of *N*-tosyl hydrazones, especially at lower temperatures.[22] The optimization studies here show that the combination of dioxane as the solvent and NaHMDS as the base had a greater impact on the reaction than the catalyst. It is worthy to note that when the catalyst loading was lowered to 2 mol %, $Rh_2(OAc)_3$(MeTOX) (**1**) outperformed both $Rh_2(OAc)_4$ and $Rh_2(OAc)_3$(2-OX) (**3**) (Table 1, compare entries 14−16).

Dioxane has been the solvent of choice for many Bamford-Stevens degradations of N-sulfonyl hydrazones in various Rh(II)-catalyzed transformations, and 1,4-dioxane has been the optimal solvent to facilitate the Bamford−Stevens degradation of a hydrazone to the reactive diazo in situ.[23] We were also interested in investigating whether solvent interactions, at axial sites of the catalyst or with the rhodium carbene intermediate, could be playing a role in the results. Axial coordination of solvents in donor-type carbene insertion reactions can have an impact on reaction outcomes,[24] and ethereal solvents have been previously used in carbene transfer reactions as both a solvent and a reactant.[25] For example, in the pursuit of macrocycles, Lacour et al. used 1,4-dioxane as both a solvent and reactant and proposed that the 1,4-dioxane attacks the Rh(II)- carbene, thereby releasing the catalyst and forming a free ylide.[23d] This ylide then experiences a [3 + 6 + 3 + 6] cyclization with another free ylide to form the desired macrocycle. This mechanism was confirmed with in situ IR and UV−vis titration experiments, which also determined that the reactive rhodium catalyst species in solution had 1,4-dioxane coordinated at one axial site.[26] We envisioned a new rhodium complex with tethered ethereal ligands to investigate the potential for 1,4-dioxane axial coordination and interaction with the transient Rh(II)-carbene in our conditions.

Ring opening of phthalic anhydride with tetrahydrofurfuryl amine **6** produced THF carbamoylbenzoic acid (THFCB) **7** in a straightforward manner in 83% yield (Figure 2a). The same reaction with dioxanylmethanamine **8** provided dioxanyl carbamoylbenzoic acid (DXCB) **9** in 43% yield. Compounds **7** and **9** were then used in ligand exchange reactions with *cis*-$Rh_2(OAc)_2(tfa)_2$ **10**[27] to produce *cis*-$Rh(OAc)_2(THFCB)_2$ complex **11** and *cis*-$Rh(OAc)_2(DXCB)_2$ complex **12** in good to excellent yields (Figure 2b). Displacement of the tfa bridging ligands in **10** occurs more readily than acetates, so subsequent ligand exchange produces solely cis-substituted Rh(II) complexes.[27,28] The disubstituted complexes **11** and **12** were targeted in order to have the potential for axial interactions at both sites of the Rh(II) complex to better mimic the influence of dioxane and THF as solvents. Even though coordination to both axial sites can reduce catalytic activity, ethereal groups generally form weak adducts with

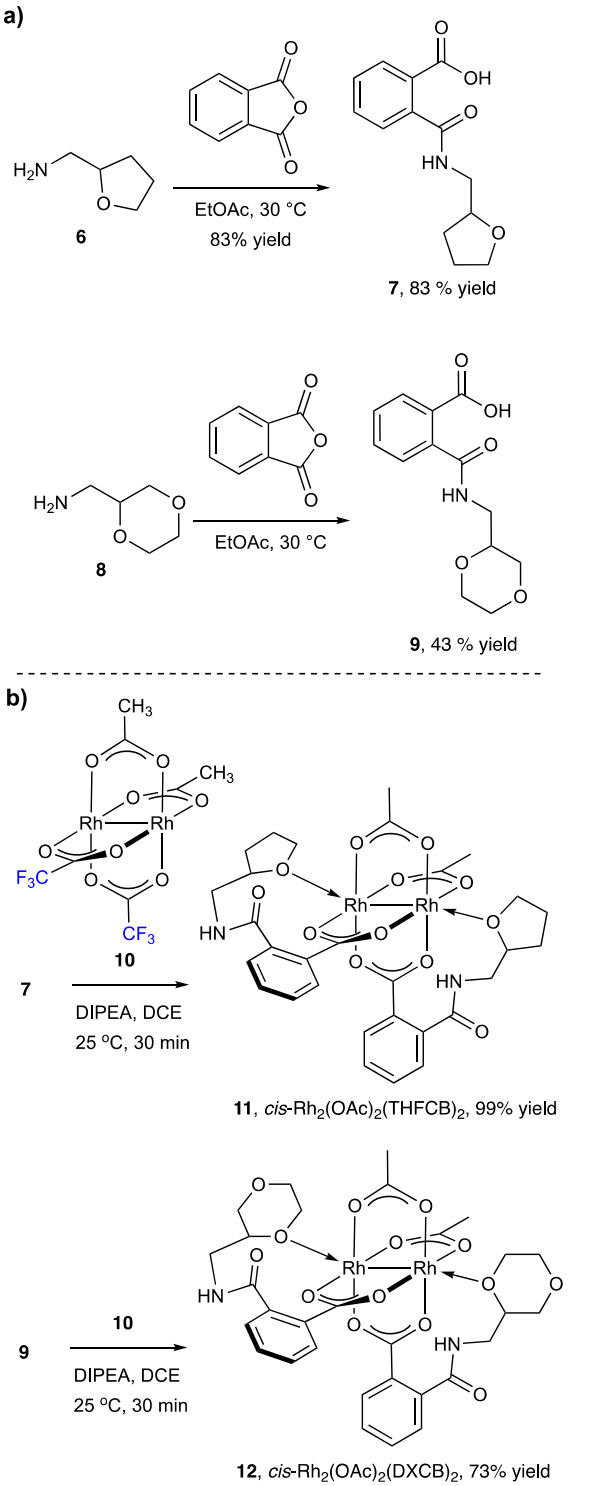

Figure 2. (a) Synthesis of THF carbamoylbenzoate (THFCB) ligand **7** and dioxanylcarbamoylbenzate (DXCB) ligand **9**. (b) Ligand exchange of **7** and **9** with $Rh_2(OAc)_2(tfa)_2$ complex **10** to produce *cis*-$Rh_2(OAc)_2(THFCB)_2$ complex **11** and *cis*-$Rh_2(OAc)_2(DXCB)_2$ complex **12**.

Rh(II) paddlewheel complexes[29] due to a hard−soft acid−base mismatch,[30] suggesting that the incorporation of ligands **7** and **9** should still allow for sufficient reactivity. It should also be noted that since ligands **7** and **9** are racemic, their respective complexes form matched or mismatched diastereomeric mixtures when exchanged (*RR*/*SS* and *SR*/*RS*). Indeed, ^{13}C

https://doi.org/10.1021/acsomega.3c03519
ACS Omega 2023, 8, 38005−38012

NMR shifts of the complexes show pairs of signals of equal intensity that signify the presence of diastereomers (see the Supporting Information).[31]

Complexes **11** and **12** were subsequently used in the model Si−H insertion reaction using DCM as the solvent to evaluate the influence of the tethered axial ligands. Complex **11** produced silyl product **5a** in a good yield (63% yield, Figure 3). By contrast, incorporation of the tethered dioxane in complex **12** provided **5a** in only 40% yield. The reversal of the tethered ligands with their respective performance as solvents could indicate that the role of dioxane precludes interaction at both axial sites to maximize yields. Although THF is considered a better inhibitor of diazo-mediated carbene transfer reactions,[32] tethering the THF tempers its inhibitory qualities. The results with complex **11** was only comparable to the 60% yield achieved with $Rh_2(OAc)_4$ in the same conditions, which indicates that ether-like axial coordination at both axial sites have minimal influence in the reaction studied here.

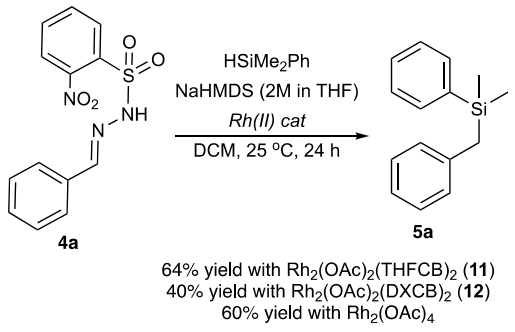

Figure 3. Synthesis of **5a** catalyzed by complexes **11** and **12** compared with $Rh_2(OAc)_4$. Yields were determined by ^{1}H NMR and are an average of 2 runs.

We moved forward to investigate the scope of reactivity with nosyl-protected, para-substituted aryl hydrazones **4a−h** to evaluate the functional group tolerance and electronic effects of this substitution (Figure 4). Since yields of the model reaction were comparable between $Rh_2(OAc)_4$ and $Rh_2(OAc)_3$(2-OX) complex **3** (Table 1 compare entries 12 and 13) and tethered complex **11**, it was more convenient to avoid synthetic steps and use the commercially available $Rh_2(OAc)_4$ for the reaction. However, when the synthesis of **5b**, **5c**, and **5d** was attempted with $Rh_2(OAc)_4$, yields were lower than expected (Figure 4). Only 14% yield was obtained for **5b**, trace yield for **5c**, and 41% yield for **5d**. Yields improved for those substrates with $Rh_2(OAc)_3$(2-OX) complex **3**, so complex **3** was used to evaluate the rest of the substrates. The electron releasing para

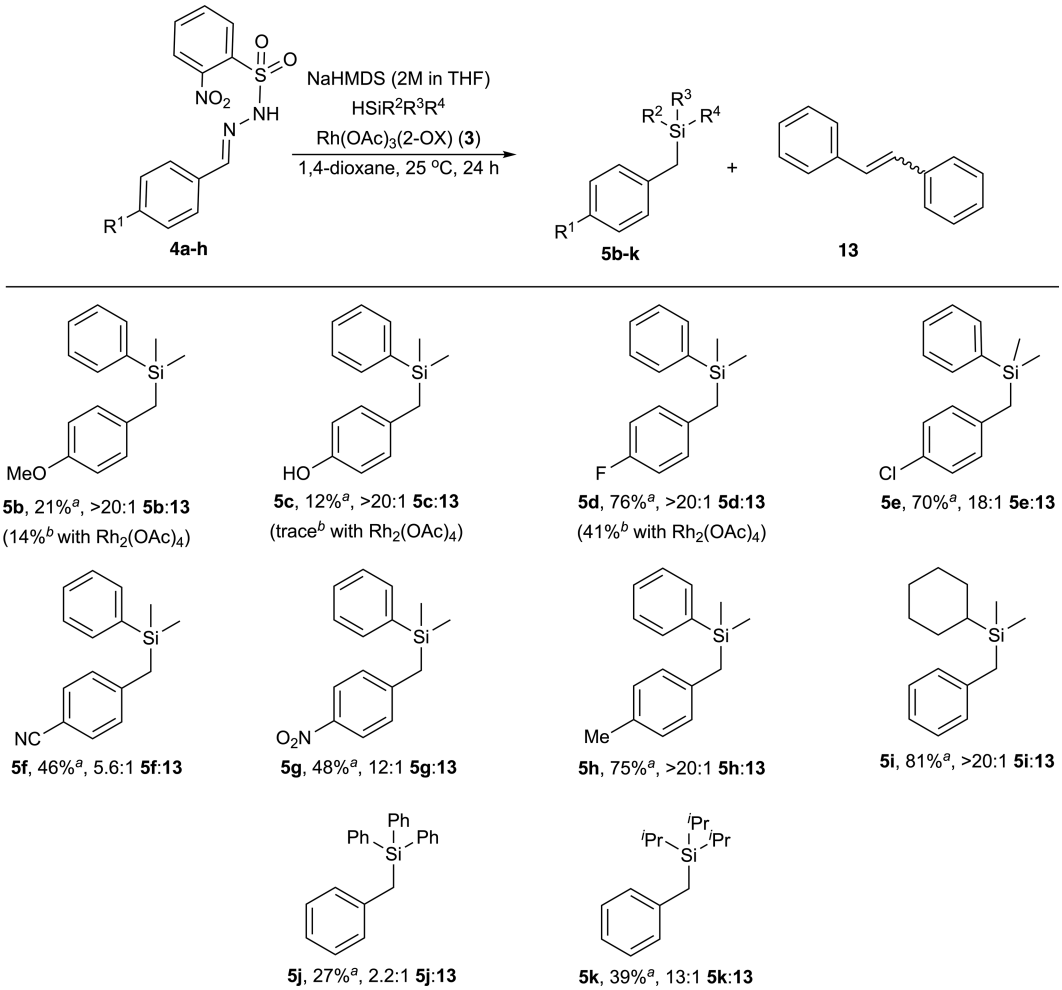

Figure 4. Substrate scope with respect to *N*-nosylhydrazones and silanes. Yields were determined by ^{1}H NMR with reference to [a] dimethyl carbonate or [b] dimethyl sulfone as the internal standard.

https://doi.org/10.1021/acsomega.3c03519
ACS Omega 2023, 8, 38005−38012

methoxy substituent negatively affected the conversion of the diazo compared to the model system, with only a 21% yield of **5b** obtained with complex **3**. This could be due to the further stabilization of the carbene intermediate by the methoxy group, resulting in decreased reactivity of the carbene. Likewise, substitution of the model substate with a para hydroxy group greatly suppressed the conversion to silane **5c** (12% yield with **3**, Figure 4) and had a more complex product distribution. The side products were not analyzed, but the competitive and relatively facile O−H insertion reaction is suspected to be partly responsible for the low yield. Halogenated substrates fared much better, with the para-fluoro-substituted hydrazone substrate affording 76% of silane product **5d** using complex **3**. The para chloro substituted hydrazone afforded 70% of silane product **5e** and an 18:1 ratio of **5e**:**13**. While formal diazo homocoupling product **13** was not observed in the model reaction, it was detectable in the production of **5e** and other reactions studied in Figure 4, which likely contributed to lower yields. The substrate with the para cyano substituent afforded a 46% yield of the silane product **5f** along with formation of the homocoupling product **13** in a 5.6:1 ratio of **5f**:**13**. The cyano group can also axially coordinate and potentially poison the catalyst or slow the rate of reaction.[34] The electron-withdrawing para-nitro substituent also gave fair yields, affording 48% of silane product **5g**. Again, the presence of the product from diazo homocoupling was observed by ^{1}H NMR in a 12:1 **5g**:**13** ratio. The para methyl substituent afforded a comparable yield of silane **5h** when compared to the model substrate (75% yield, Figure 4). Other silanes were also evaluated in the reaction. The reaction with **4a** and cyclohexyl(dimethyl) silane afforded its respective insertion product smoothly in 80% yield. There was a drop in yield when more sterically demanding silanes **5j** and **5k** were used, resulting in 27 and 39% yields, respectively (Figure 4).

CONCLUSIONS

In summary, we have found that nosyl-protected hydrazones coupled with NaHMDS as a base and dioxane as the solvent are suitable conditions to facilitate Rh(II)-catalyzed Si−H insertion reactions. $Rh_2(OAc)_3$(2-OX) (**3**) was the optimal catalyst based on product yield when compared to other tested catalysts, although rhodium catalyst **1** with TACLs was better at lower catalyst loading. The combination of base and solvent had the greatest positive effect on this transformation, and elevated temperatures had a negative impact on the transformation. Lastly, the transformation was sensitive to the functional group change at the para position. Rh(II)-catalyzed Si−H insertions with hydrazones as diazo precursors often suffer from low yields,[7] but the promising results of this study highlights that with the right conditions, Rh(II) catalysts are viable in Si−H insertions with hydrazone protected donor diazo compounds. The investigation of Rh(II) complexes with tethered axial coordination hints at a minimal effect of axial coordination for producing good yields. However, the ease of synthesis of complexes and the interesting role reversals between solvent and tethered axial ligand begs further inspection of tethered oxygen ligand coordination[33] in Rh(II)-catalyzed reactions in future studies. The development of more of these complexes and strategies to broaden the scope of Si−H insertion reactions is underway in our laboratory.

EXPERIMENTAL SECTION

Materials and Methods. Unless otherwise noted, all reagents were purchased and used as received from the manufacturer without further purification. Complexes $Rh_2(OAc)_3$(MeTOX) (**1**),[35] $Rh_2(OAc)_3$(PhTOX) (**2**),[36] $Rh_2(OAc)_3$(OX) (**3**),[17] and $Rh_2(OAc)_2(tfa)_2$ (**10**)[27] were synthesized via established literature procedures. 1,2-Dichloroethane (DCE), dichloromethane (DCM), tetrahydrofuran (THF), 1,4-dioxane, and acetonitrile (ACN) were used as received from vendors unless otherwise noted. Column chromatography was performed using 60 Å, 40−63 μm silica from Sorbent Technologies. ^{1}H and ^{13}C NMR spectra were recorded on Varian Mercury Vx 300 MHz or Bruker AVANCE NEO 500 MHz spectrometers. All ^{1}H and ^{13}C NMR chemical shifts are reported in parts per million on the δ scale. Signals were referenced by the residual solvent signal for ^{1}H NMR ($CHCl_3$ = 7.26 ppm, DMSO = 2.50 ppm, CD_3CN = 1.94 ppm) and ^{13}C NMR ($CHCl_3$ = 77.16 ppm, DMSO = 39.52 ppm, CD_3CN = 1.32 ppm). The mass spectra for compounds were obtained using an AccuTOF Mass spectrometer equipped with a direct analysis in real time (DART) ionization apparatus. The mass spectra for complexes **11** and **12** was obtained using a Water SYNAPT G2-*Si* MALDI-TOF Mass Spectrometer. Elemental analyses were performed by Atlantic Microlab (Norcross, GA). Hydrazones **4a**, **4a'**, **4b**, and **4d**−**h** were made from established literature procedures.[37]

***N*-(4-Hydroxybenzylidene)-2-nitrobenzenesulfonohydrazide (4c).** 4-Hydroxybenaldehyde (300 mg, 1.38 mmol) was added to a 25 mL round-bottom flask fitted with a magnetic stirbar and dissolved in ethanol (0.7 mL). 2-Nitrobenzenesulfonohydrazide (177.1 mg, 1.45 mmol) and acetic acid (3.95 μL, 69.1 μmol) were then added sequentially, resulting in a brown solution. The round-bottom flask was then fitted with a septum and vented with a needle. The solution was stirred at ambient temperature for 2 h at which point the solution turned orange. The volume of the solution was reduced in vacuo. Hexanes (3 mL) were added to the residue to precipitate an orange solid that was filtered and further rinsed with hexanes to obtain the pure product (410.7 mg, 93% yield). ^{1}H NMR (DMSO-d_6, 500 MHz): δ 11.78 (s, 1H, S−N*H*−N), 9.90 (s, 1H, −O*H*), 8.04−8.03 (m, 1H, Ar−*H*), 8.01−7.97 (m, 1H, Ar−*H*), 7.96 (s, 1H, N=C*H*−), 7.90−7.85 (m, 2H, Ar−*H*), 7.40 (d, 2H, J = 8.7 Hz, Ar−*H*), 6.76 (d, 2H, J = 8.7 Hz, Ar−*H*). ^{13}C{^{1}H} NMR (125 MHz, DMSO-d_6): δ 159.6, 148.2, 147.9, 134.6, 132.5, 131.1, 130.4, 128.7, 124.4, 124.4, 115.6. Anal. Calcd for $C_{13}H_{11}N_3O_5S$: C, 48.60; H, 3.45; N, 13.08; S, 9.98. Found: C, 49.65; H, 3.52; N, 12.43; S, 9.57.

General Procedure for Si−H Insertion. Hydrazone (0.75 mL from a 0.09 M stock solution, 0.065 mmol) was added in one portion to a 2−5 mL microwave reaction vial fitted with a magnetic stir bar. Base (0.098 mmol) was then added, and the mixture was stirred for approximately 5 min. Silane (0.328 mmol) and rhodium catalyst (0.5 mL from a 0.0065 M stock solution, 5 mol %) were added sequentially in that order. The vial was immediately capped, crimped, and placed in a preheated aluminum well plate set to 25 °C. The reaction mixture was stirred for 24 h and then filtered through a 1 cm × 0.5 cm column of silica gel to remove Sulphone salt using DCM (25 mL) to elute the material into a 50 mL round-bottom flask. Excess solvent was removed by rotary evaporation and the crude material was dissolved in chloroform-*d*. Mesitylene (0.065 mmol), dimethyl carbonate (0.065

https://doi.org/10.1021/acsomega.3c03519
ACS Omega 2023, 8, 38005−38012

mmol), or dimethyl sulfone (0.065 mmol) was added as an internal standard. Yields were obtained via ^{1}H NMR. Chemical shifts of known products matched what was reported in literature.[38]

Silyl Product Yield Calculations. Normalized integration of the methyl proton signal of mesitylene (2.28 ppm), dimethyl carbonate (3.79 ppm), or dimethyl sulfone (3.00 ppm) was compared to the integration of the protons assigned to the methylene of the silane products.

4-((Dimethyl(phenyl)silyl)methyl)phenol (5c). Yield 12%; colorless oil; ^{1}H NMR ($CDCl_3$, 500 MHz): δ 7.46−7.44 (m, 2H, Ar−*H*), 7.36−7.32 (m, 3H, Ar−*H*), 6.79 (d, 2H, J = 8.6 Hz, Ar−*H*), 6.83 (d, 2H, J = 8.6 Hz, Ar−*H*), 2.22 (s, 2H, −CH_2−), 0.23 (s, 6H, −CH_3). ^{13}C{^{1}H} NMR ($CDCl_3$, 125 MHz): δ 152.5, 138.7, 133.9, 131.8, 129.4, 129.2, 128.7, 127.8, 126.2, 115.2, 25.0, −3.3. HRMS (DART) m/z calcd. for $C_{15}H_{18}O_8Si$ $[M]^+$ 242.1127, found 242.0956.

(4-Chlorobenzyl)dimethyl(phenyl)silane (5e). Yield 70%; colorless oil; ^{1}H NMR ($CDCl_3$, 500 MHz): δ 7.44−7.42 (m, 2H, Ar−*H*), 7.37−7.33 (m, 3H, Ar−*H*), 7.13 (d, 2H, J = 8.4 Hz, Ar−*H*), 6.83 (d, 2H, J = 8.4 Hz, Ar−*H*), 2.26 (s, 2H, −CH_2−), 0.25 (s, 6H, −CH_3). ^{13}C{^{1}H} NMR ($CDCl_3$, 125 MHz): δ 138.4, 138.1, 133.8, 129.9, 129.7, 129.3, 128.7, 128.3, 127.9, 25.9, −3.42. Anal. Calcd for $C_{15}H_{17}ClSi$: C, 69.07; H, 6.57. Found: C, 68.79; H, 6.44.

(4-Nitrobenzyl)dimethyl(phenyl)silane (5g). Yield 48%; yellow solid; ^{1}H NMR ($CDCl_3$, 500 MHz): δ 8.02 (d, 2H, J = 8.9 Hz, Ar−*H*), 7.41−7.33 (m, 5H, Ar−*H*), 6.99 (d, 2H, J = 8.9 Hz, Ar−*H*), 2.44 (s, 2H, −CH_2−), 0.29 (s, 6H, −CH_3). ^{13}C{^{1}H} NMR ($CDCl_3$, 125 MHz): δ 148.9, 145.2, 137.0, 133.8, 129.7, 128.7, 128.1, 123.7, 27.8, −3.5. HRMS (DART) m/z calcd. for $C_{15}H_{17}NO_2Si$ $[M]^+$ 271.1029, found 271.1084.

2-(((Tetrahydrofuran-2-yl)methyl)carbamoyl)benzoic Acid (7). A round-bottom flask was equipped with a magnetic stir bar, and tetrahydrofurfuryl amine **6** (1.02 g, 10.0 mmol) was added. Ethyl acetate (7 mL) was added and the solution was stirred. Phthalic anhydride (1.50 g, 10.0 mmol) was added in portions and the resulting clear, colorless solution was stirred at 30 °C for 2 h, after which TLC showed that the reaction was complete. The mixture was concentrated via reduced pressure, and the residue was recrystallized with ethyl acetate to obtain compound **7** as a white solid in 83% yield (2.08 g, 8.34 mmol). ^{1}H NMR ($CDCl_3$, 500 MHz,) δ 8.03 (dd, J = 8.1, 1.4 Hz, 1H), 7.61−7.54 (m, 1H), 7.54−7.48 (m, 2H), 6.86 (s, 1H), 4.16 (qd, J = 7.3, 3.0 Hz, 1H), 3.87 (m, 2H), 3.83−3.76 (m, 1H), 3.29 (m, 1H), 2.14−2.03 (m, 1H), 1.95 (m, 2H), 1.72−1.60 (m, 1H). ^{13}C{^{1}H} NMR ($CDCl_3$, 126 MHz,) δ: 171.1, 168.3, 136.6, 132.4, 132.3, 130.5, 129.9, 127.9, 77.8, 68.3, 44.3, 28.9, 25.9. Anal. Calcd for $C_{13}H_{15}NO_4$: C, 62.64; H, 6.07; N, 5.62. Found: C, 62.08; H, 6.07; N, 5.47.

2-(((1,4-Dioxan-2-yl)methyl)carbamoyl)benzoic Acid (9). A round-bottom flask was equipped with a magnetic stir bar, and dioxanylmethanamine **8** (0.200 g, 1.70 mmol) was added. Ethyl acetate (1.2 mL) was added and the solution was stirred. Phthalic anhydride (0.253 g, 1.70 mmol) was added in portions and the resulting clear, colorless solution was stirred at 30 °C for 30 min, after which white solids precipitated from the solution and TLC showed that the reaction was complete. The residue was recrystallized with ethyl acetate to obtain compound **9** as a white solid in 43% yield (0.192 g, 0.725 mmol). ^{1}H NMR (500 MHz, CD_3CN) δ 7.88 (dd, J = 7.8, 1.4 Hz, 1H), 7.59 (td, J = 7.5, 1.4 Hz, 1H), 7.53 (td, J = 7.6, 1.4 Hz, 1H), 7.47 (dd, J = 7.6, 1.4 Hz, 1H), 6.98 (s, 1H), 3.80 (dd, J = 11.5, 2.6 Hz, 1H), 3.77−3.61 (m, 4H), 3.52 (td, J = 11.1, 2.8 Hz, 1H), 3.41−3.26 (m, 3H). ^{13}C NMR (126 MHz, CD_3CN) δ: 170.6, 168.2, 138.6, 132.8, 131.3, 130.9, 130.8, 128.8, 74.7, 69.9, 67.4, 67.0, 41.6. HRMS (ESI-TOF) m/z: $[M - H]^-$ Calcd for $C_{13}H_{14}NO_5$ 264.0872, Found 264.0869.

***cis*-$Rh_2(OAc)_2(THFCB)_2$ (11).** To a 20 mL vial with a threaded top were added $Rh_2(OAc)_2(tfa)_2$ (40 mg, 0.073 mmol) and 1,2-dichloroethane (DCE, 10 mL). Compound **7** (36 mg, 0.145 mmol) was then added in one portion to the vial, and the mixture stirred. Diisopropylethylamine (29 mg, 0.224 mmol) was weighed in a separate vial and transferred with 4 mL DCE. The mixture was stirred at 50 °C for 30 min, at which point TLC showed that the reaction was complete. The mixture was concentrated under reduced pressure, and the residue was purified by column chromatography using 2% methanol in dichloromethane as the eluent to produce complex **11** as a green solid in quantitative yield (60 mg, 0.073 mmol). ^{1}H NMR (CD_3CN, 500 MHz,) δ 7.48 (d, J = 7.6 Hz, 2H), 7.41 (td, J = 7.5, 1.5 Hz, 2H), 7.35 (td, J = 7.5, 1.4 Hz, 2H), 7.27 (dd, J = 7.5, 1.3 Hz, 2H), 7.05 (dt, J = 12.2, 5.8 Hz, 2H), 3.69 (m, 2H), 3.57 (m, 2H), 3.48−3.37 (m, 2H), 3.21−3.01 (m, 4H), 1.82 (s, 6H), 1.78−1.59 (m, 6H), 1.41−1.23 (m, 3H). ^{13}C{^{1}H} NMR (CD_3CN, 126 MHz) δ: 192.4, 187.2, 170.3, 137.9, 131.0, 129.8, 128.0, 128.8, 128.1, 78.2, 78.2, 68.2, 68.2, 44.6, 44.6, 29.7, 29.6, 26.3, 26.2, 23.7. HRMS (ESI-TOF) m/z: $[M + Na]^+$ Calcd for $C_{30}H_{34}NaN_2O_{12}Rh_2$ 843.0120, Found 843.0103.

***cis*-$Rh_2(OAc)_2(DXCB)_2$ (12).** To a 20 mL vial with a threaded top were added $Rh_2(OAc)_2(tfa)_2$ (24 mg, 0.044 mmol) and 1,2-dichloroethane (DCE, 5 mL). Compound **9** (23 mg, 0.087 mmol) was then added in one portion to the vial, and the mixture stirred. Diisopropylethylamine (23 mg, 0.174 mmol) was weighed in a separate vial and transferred with 5 mL DCE. The mixture was stirred at 50 °C for 30 min, at which point TLC showed that the reaction was complete. The mixture was concentrated under reduced pressure, and the residue was purified by column chromatography using 2% methanol in dichloromethane as the eluent to produce complex **12** as a green solid in 73% yield (27 mg, 0.032 mmol). ^{1}H NMR (500 MHz, CD_3CN) δ 7.48 (d, J = 7.6 Hz, 2H), 7.42 (t, J = 7.5 Hz, 2H), 7.37 (t, J = 6.9 Hz, 2H), 7.28 (d, J = 7.5 Hz, 2H), 7.12 (m, 2H), 3.62−3.47 (m, 7H), 3.45−3.25 (m, 7H), 3.14−2.96 (m, 7H), 1.82 (s, 6H). ^{13}C NMR (126 MHz, CD_3CN) δ 192.4, 187.3, 170.5, 170.4, 137.6, 133.8, 131.1, 131.1, 130.1, 128.9, 128.9, 128.1, 128.0, 74.5, 74.5, 70.03, 70.01, 67.03, 66.99, 66.92, 66.90, 41.68, 41.65, 23.7. HRMS (MALDI-TOF) m/z: $[M + Na]^+$ Calcd for $C_{30}H_{34}NaN_2O_{14}Rh_2$ 875.0018, Found 875.0020.

■ ASSOCIATED CONTENT

Supporting Information

The Supporting Information is available free of charge at https://pubs.acs.org/doi/10.1021/acsomega.3c03519.

NMR spectra for **4c**, **5c**, **5e**, **5g**, **7**, **9**, **11**, and **12** (PDF)

FAIR data, including the primary NMR FID files, for **4c**, **5c**, **5e**, and **5g** (ZIP)

■ AUTHOR INFORMATION

Corresponding Author

Ampofo Darko − *Department of Chemistry, University of Tennessee, Knoxville, Tennessee 37996, United States;*

https://doi.org/10.1021/acsomega.3c03519
ACS Omega 2023, 8, 38005−38012

orcid.org/0000-0003-1725-4907; Email: adarko@utk.edu

Authors

Anthony Abshire − *Department of Chemistry, University of Tennessee, Knoxville, Tennessee 37996, United States*

Bukola Ogunyemi − *Department of Chemistry, University of Tennessee, Knoxville, Tennessee 37996, United States*

Complete contact information is available at: https://pubs.acs.org/10.1021/acsomega.3c03519

Author Contributions

All authors have given approval to the final version of the manuscript.

Notes

The authors declare no competing financial interest.

The data underlying this study are available in the published article and its online Supporting Information.

■ ACKNOWLEDGMENTS

The authors thank the University of Tennessee, Knoxville for their generous support. The authors also thank the personnel in the NMR facilities and the Biological and Small Molecule Mass Spectrometry Core facilities at the University of Tennessee. Funding for open access to this research was provided by University of Tennessee's Open Publishing Support Fund.

■ REFERENCES

(1) (a) Davies, H. M. L.; Antoulinakis, E. G. Intermolecular metal-catalyzed carbenoid cyclopropanations. *Org. React. (N. Y.)* **2001**, *57*, 1−326. (b) Chepiga, K. M.; Qin, C.; Alford, J. S.; Chennamadhavuni, S.; Gregg, T. M.; Olson, J. P.; Davies, H. M. L. Guide to enantioselective dirhodium(II)-catalyzed cyclopropanation with aryldiazoacetates. *Tetrahedron* **2013**, *69* (27−28), 5765−5771.

(2) (a) Davies, H. M. L.; Morton, D. Guiding principles for site selective and stereoselective intermolecular C−H functionalization by donor/acceptor rhodium carbenes. *Chem. Soc. Rev.* **2011**, *40* (4), 1857−1869. (b) Keipour, H.; Carreras, V.; Ollevier, T. Recent progress in the catalytic carbene insertion reactions into the silicon−hydrogen bond. *Org. Biomol. Chem.* **2017**, *15* (26), 5441−5456. (c) Paulissen, R.; Reimlinger, H.; Hayez, E.; Hubert, A. J.; Teyssie, P. Transition metal catalyzed reactions of diazo compounds. II. Insertion in the hydroxylic bond. *Tetrahedron Lett.* **1973**, *24*, 2233. (d) Gillingham, D.; Fei, N. Catalytic X−H insertion reactions based on carbenoids. *Chem. Soc. Rev.* **2013**, *42* (12), 4918−4931. (e) Pang, Y.; He, Q.; Li, Z.-Q.; Yang, J.-M.; Yu, J.-H.; Zhu, S.-F.; Zhou, Q.-L. Rhodium-Catalyzed B−H Bond Insertion Reactions of Unstabilized Diazo Compounds Generated in Situ from Tosylhydrazones. *J. Am. Chem. Soc.* **2018**, *140* (34), 10663−10668.

(3) (a) Jinnouchi, H.; Nambu, H.; Takahashi, K.; Fujiwara, T.; Yakura, T. Chemo- and stereoselective six-membered oxonium ylide formation−[2,3]-sigmatropic rearrangement of 2-diazo-3-ketoesters with dirhodium(II) catalyst and its application to the synthesis of (+)-tanikolide. *Tetrahedron* **2019**, *75* (16), 2436−2445. (b) Sheng, Z.; Zhang, Z.; Chu, C.; Zhang, Y.; Wang, J. Transition metal-catalyzed [2,3]-sigmatropic rearrangements of ylides: An update of the most recent advances. *Tetrahedron* **2017**, *73* (29), 4011−4022.

(4) (a) Zhu, D.; Chen, L.; Fan, H.; Yao, Q.; Zhu, S. Recent progress on donor and donor-donor carbenes. *Chem. Soc. Rev.* **2020**, *49* (3), 908−950. (b) Green, S. P.; Wheelhouse, K. M.; Payne, A. D.; Hallett, J. P.; Miller, P. W.; Bull, J. A. Thermal Stability and Explosive Hazard Assessment of Diazo Compounds and Diazo Transfer Reagents. *Org. Process Res. Dev.* **2020**, *24* (1), 67−84.

(5) Ghavre, M. Bamford-Stevens and Shapiro Reactions in Organic Synthesis. *Asian J. Org. Chem.* **2020**, *9* (12), 1901−1923.

(6) Werlé, C.; Goddard, R.; Fürstner, A. The First Crystal Structure of a Reactive Dirhodium Carbene Complex and a Versatile Method for the Preparation of Gold Carbenes by Rhodium-to-Gold Transmetalation. *Angew. Chem., Int. Ed.* **2015**, *54* (51), 15452−15456.

(7) Liu, Z.; Li, Q.; Yang, Y.; Bi, X. Silver(I)-promoted insertion into X−H (X = Si, Sn, and Ge) bonds with *N*-nosylhydrazones. *Chem. Commun.* **2017**, *53* (16), 2503−2506.

(8) Wang, E.-H.; Ping, Y.-J.; Li, Z.-R.; Qin, H.; Xu, Z.-J.; Che, C.-M. Iron Porphyrin Catalyzed Insertion Reaction of N-Tosylhydrazone-Derived Carbenes into X−H (X = Si, Sn, Ge) Bonds. *Org. Lett.* **2018**, *20* (15), 4641−4644.

(9) Liu, Z.; Huo, J.; Fu, T.; Tan, H.; Ye, F.; Hossain, M. L.; Wang, J. Palladium(0)-catalyzed C(sp^3)−Si bond formation via formal carbene insertion into a Si−H bond. *Chem. Commun.* **2018**, *54* (81), 11419−11422.

(10) Kramer, K. A. W.; Wright, A. N. Reaction of Diazoalkanes with Group IV Hydrides. *J. Chem. Soc.* **1963**, 3604−3608.

(11) Bagheri, V.; Doyle, M. P.; Taunton, J.; Claxton, E. E. A New and General-Synthesis of α-Silyl Carbonyl-Compounds by Si−H Insertion from Transition-Metal Catalyzed-Reactions of Diazo Esters and Diazo Ketones. *J. Org. Chem.* **1988**, *53* (26), 6158−6160.

(12) Keipour, H.; Carreras, V.; Ollevier, T. Recent progress in the catalytic carbene insertion reactions into the silicon-hydrogen bond. *Org. Biomol. Chem.* **2017**, *15* (26), 5441−5456.

(13) (a) Chabaud, L.; James, P.; Landais, Y. Allylsilanes in organic synthesis - Recent developments. *Eur. J. Org. Chem.* **2004**, *15*, 3173−3199, DOI: 10.1002/ejoc.200300789. (b) Landais, Y.; Planchenault, D. Preparation of optically active α-silylcarbonyl compounds using asymmetric alkylation of α-silylacetic esters and asymmetric metal-carbene insertion into the Si−H bond. *Tetrahedron* **1997**, *53* (8), 2855−2870. (c) Landais, Y.; ParraRapado, L.; Planchenault, D.; Weber, V. Mechanism of metal-carbenoid insertion into the Si-H bond. *Tetrahedron Lett.* **1997**, *38* (2), 229−232.

(14) Kitagaki, S.; Kinoshita, M.; Takeba, M.; Anada, M.; Hashimoto, S. Enantioselective Si−H insertion of methyl phenyldiazoacetate catalyzed by dirhodium(II) carboxylates incorporating *N*-phthaloyl-(*S*)-amino acids as chiral bridging ligands. *Tetrahedron: Asymmetry* **2000**, *11* (19), 3855−3859.

(15) (a) Sambasivan, R.; Ball, Z. T. Determination of orientational isomerism in rhodium(II) metallopeptides by pyrene fluorescence. *Org. Biomol. Chem.* **2012**, *10* (41), 8203−8206. (b) Zaykov, A. N.; Ball, Z. T. Kinetic and stereoselectivity effects of phosphite ligands in dirhodium catalysis. *Tetrahedron* **2011**, *67* (24), 4397−4401. (c) Sambasivan, R.; Ball, Z. T. Metallopeptides for Asymmetric Dirhodium Catalysis. *J. Am. Chem. Soc.* **2010**, *132* (27), 9289−9291.

(16) (a) Jagannathan, J. R.; Fettinger, J. C.; Shaw, J. T.; Franz, A. K. Enantioselective Si−H Insertion Reactions of Diarylcarbenes for the Synthesis of Silicon-Stereogenic Silanes. *J. Am. Chem. Soc.* **2020**, *142* (27), 11674−11679. (b) Huang, M. Y.; Yang, J. M.; Zhao, Y. T.; Zhu, S. F. Rhodium-Catalyzed Si−H Bond Insertion Reactions Using Functionalized Alkynes as Carbene Precursors. *ACS Catal.* **2019**, *9* (6), 5353−5357.

(17) Sheffield, W.; Abshire, A.; Darko, A. Effect of Tethered, Axial Thioether Coordination on Rhodium(II)-Catalyzed Silyl-Hydrogen Insertion. *Eur. J. Org. Chem.* **2019**, *2019* (37), 6347−6351.

(18) (a) Wei, B.; Sharland, J. C.; Blackmond, D. G.; Musaev, D. G.; Davies, H. M. L. In Situ Kinetic Studies of Rh(II)-Catalyzed C−H Functionalization to Achieve High Catalyst Turnover Numbers. *ACS Catal.* **2022**, *12* (21), 13400−13410. (b) Wei, B.; Sharland, J. C.; Lin, P.; Wilkerson-Hill, S. M.; Fullilove, F. A.; McKinnon, S.; Blackmond, D. G.; Davies, H. M. L. In Situ Kinetic Studies of Rh(II)-Catalyzed Asymmetric Cyclopropanation with Low Catalyst Loadings. *ACS Catal.* **2020**, *10* (2), 1161−1170.

(19) (a) Feng, J.-J.; Oestreich, M. Tertiary α-Silyl Alcohols by Diastereoselective Coupling of 1,3-Dienes and Acylsilanes Initiated by Enantioselective Copper-Catalyzed Borylation. *Angew. Chem., Int. Ed.* **2019**, *58* (24), 8211−8215. (b) Huckins, J. R.; Rychnovsky, S. D. Synthesis of Optically Pure Arylsilylcarbinols and Their Use as Chiral

Auxiliaries in Oxacarbenium Ion Reactions. *J. Org. Chem.* **2003**, *68* (26), 10135−10145.
(20) Uyanik, M.; Mutsuga, T.; Ishihara, K. 4,5-Dimethyl-2-Iodoxybenzenesulfonic Acid Catalyzed Site-Selective Oxidation of 2-Substituted Phenols to 1,2-Quinols. *Angew. Chem., Int. Ed.* **2017**, *56* (14), 3956−3960.
(21) Pruchnik, F. P. Structure and reactivity of rhodium(II) complexes. *Pure Appl. Chem.* **1989**, *61* (5), 795−804.
(22) Liu, Z.; Raveendra Babu, K.; Wang, F.; Yang, Y.; Bi, X. Influence of sulfonyl substituents on the decomposition of *N*-sulfonylhydrazones at room temperature. *Org. Chem. Front.* **2019**, *6* (1), 121−124.
(23) (a) Li, Y.; Huang, Z.; Wu, X.; Xu, P.-F.; Jin, J.; Zhang, Y.; Wang, J. Rh(II)-catalyzed [2,3]-sigmatropic rearrangement of sulfur ylides derived from N-tosylhydrazones and sulfides. *Tetrahedron* **2012**, *68* (26), 5234−5240. (b) Le, P. Q.; May, J. A. Hydrazone-Initiated Carbene/Alkyne Cascades to Form Polycyclic Products: Ring-Fused Cyclopropenes as Mechanistic Intermediates. *J. Am. Chem. Soc.* **2015**, *137* (38), 12219−12222. (c) Lingayya, R.; Vellakkaran, M.; Nagaiah, K.; Nanubolu, J. B. Rhodium(II)-Catalyzed Carbenoid Insertion of N-Tosylhydrazones into Amide N−H Bonds: An Efficient Approach to N3-Benzyl/Alkyl-2-arylquinazolinones. *Adv. Synth. Catal.* **2016**, *358* (1), 81−89. (d) Zeghida, W.; Besnard, C.; Lacour, J. Rhodium(II)-Catalyzed One-Pot Four-Component Synthesis of Functionalized Polyether Macrocycles at High Concentration. *Angew. Chem., Int. Ed.* **2010**, *49* (40), 7253−7256. (e) Medina, F.; Besnard, C.; Lacour, J. One-Step Synthesis of Nitrogen-Containing Medium-Sized Rings via α-Imino Diazo Intermediates. *Org. Lett.* **2014**, *16* (12), 3232−3235. (f) Su, N.; Deng, T.; Wink, D. J.; Driver, T. G. Achieving Site Selectivity in Metal-Catalyzed Electron-Rich Carbene Transfer Reactions from N-Tosylhydrazones. *Org. Lett.* **2017**, *19* (15), 3990−3993.
(24) Laconsay, C. J.; Pla-Quintana, A.; Tantillo, D. J. Effects of Axial Solvent Coordination to Dirhodium Complexes on the Reactivity and Selectivity in C−H Insertion Reactions: A Computational Study. *Organometallics* **2021**, *40*, 4120.
(25) (a) Du, Z.; Chen, Z.; Chen, Z.; Yu, X.; Hu, W. Dirhodium-catalyzed enantioselective C−H insertion of N-(2-benzyloxyethyl)-N-(tert-butyl)diazoacetamide and its application for the synthesis of chiral GABOB. *Chirality* **2004**, *16* (8), 516−519. (b) Liu, W.-J.; Chen, Z.-L.; Chen, Z.-Y.; Hu, W.-H. Dirhodium catalyzed intramolecular enantioselective C−H insertion reaction of N-cumyl-N-(2-p-anisylethyl)diazoacetamide: synthesis of (−)-Rolipram. *Tetrahedron: Asymmetry* **2005**, *16* (9), 1693−1698.
(26) Poggiali, D.; Homberg, A.; Lathion, T.; Piguet, C.; Lacour, J. Kinetics of Rh(II)-Catalyzed α-Diazo-β-ketoester Decomposition and Application to the [3 + 6+3 + 6] Synthesis of Macrocycles on a Large Scale and at Low Catalyst Loadings. *ACS Catal.* **2016**, *6* (8), 4877−4881.
(27) Lou, Y.; Remarchuk, T. P.; Corey, E. J. Catalysis of Enantioselective [2 + 1]-Cycloaddition Reactions of Ethyl Diazoacetate and Terminal Acetylenes Using Mixed-Ligand Complexes of the Series $Rh_2(RCO_2)_n$ (L^*_{4-n}). Stereochemical Heuristics for Ligand Exchange and Catalyst Synthesis. *J. Am. Chem. Soc.* **2005**, *127* (41), 14223−14230.
(28) (a) Minus, M. B.; Wang, H.; Munoz, J. O.; Stevens, A. M.; Mangubat-Medina, A. E.; Krueger, M. J.; Liu, W.; Kasembeli, M. M.; Cooper, J. C.; Kolosov, M. I.; et al. Targeting STAT3 anti-apoptosis pathways with organic and hybrid organic−inorganic inhibitors. *Org. Biomol. Chem.* **2020**, *18* (17), 3288−3296. (b) Minus, M. B.; Kang, M. K.; Knudsen, S. E.; Liu, W.; Krueger, M. J.; Smith, M. L.; Redell, M. S.; Ball, Z. T. Assessing the intracellular fate of rhodium(ii) complexes. *Chem. Commun.* **2016**, *52* (78), 11685−11688.
(29) (a) Mattiza, J. T.; Meyer, V. J.; Duddeck, H. Experimental verification of diverging mechanisms in the binding of ether, thioether, and sulfone ligands to a dirhodium tetracarboxylate. *Magn. Reson. Chem.* **2010**, *48* (3), 192−197. (b) Gómez, E. D.; Duddeck, H. Origin of ^{13}C complexation shifts in the adduct formation of 2-butyl phenyl ethers with a dirhodium tetracarboxylate complex. *Magn. Reson. Chem.* **2008**, *46* (1), 23−29. (c) Duddeck, H. $Rh_2[MTPA]_4$, a dirhodium complex as NMR auxiliary for chiral recognition. *Chem. Rec.* **2005**, *5* (6), 396−409.
(30) Woodward, S. HSAB matching and mismatching in selective catalysis and synthesis. *Tetrahedron* **2002**, *58* (6), 1017−1050.
(31) Pavia, A. A.; Lacombe, J. M. Carbon-13 NMR spectroscopy, a useful tool to determine the enantiomeric purity of synthetic threonine-containing glycopeptides. Spectra of diastereoisomeric.alpha.- and.beta.-D-galactopyranosyl-L- and D-threonine and -L- and -D-allothreonine. *J. Org. Chem.* **1983**, *48* (15), 2564−2568.
(32) (a) Pirrung, M. C.; Liu, H.; Morehead, A. T. Rhodium Chemzymes: Michaelis−Menten Kinetics in Dirhodium(II) Carboxylate-Catalyzed Carbenoid Reactions. *J. Am. Chem. Soc.* **2002**, *124* (6), 1014−1023. (b) Pirrung, M. C.; Morehead, A. T. Saturation Kinetics in Dirhodium(II) Carboxylate-Catalyzed Decompositions of Diazo Compounds. *J. Am. Chem. Soc.* **1996**, *118* (34), 8162−8163.
(33) Lahuerta, P.; Perez-Prieto, J.; Stiriba, S. E.; Ubeda, M. A. Novel unsymmetrical ortho-metalated dirhodium (II) catalysts: Trans influence of the axial ligand. *Tetrahedron Lett.* **1999**, *40* (9), 1751−1754.
(34) (a) Drago, R. S.; Long, J. R.; Cosmano, R. Comparison of the coordination chemistry and inductive transfer through the metal-metal bond in adducts of dirhodium and dimolybdenum carboxylates. *Inorg. Chem.* **1982**, *21* (6), 2196−2202. (b) Das, K.; Kadish, K. M.; Bear, J. L. Substituent and solvent effects on the electrochemical properties of tetra-μ-carboxylato-dirhodium(II). *Inorg. Chem.* **1978**, *17* (4), 930. (c) Chavan, M. Y.; Zhu, T. P.; Lin, X. Q.; Ahsan, M. Q.; Bear, J. L.; Kadish, K. M. Axial-ligand-dependent electrochemical and spectral properties of a series of acetate- and acetamidate-bridged dirhodium complexes. *Inorg. Chem.* **1984**, *23* (26), 4538.
(35) Anderson, B. G.; Cressy, D.; Patel, J. J.; Harris, C. F.; Yap, G. P. A.; Berry, J. F.; Darko, A. Synthesis and Catalytic Properties of Dirhodium Paddlewheel Complexes with Tethered Axially Coordinating Thioether Ligands. *Inorg. Chem.* **2019**, *58* (3), 1728−1732.
(36) Cressy, D.; Zavala, C.; Abshire, A.; Sheffield, W.; Darko, A. Tuning Rh(II)-catalysed cyclopropanation with tethered thioether ligands. *Dalton Trans.* **2020**, *49* (44), 15779−15787.
(37) Liu, Z.; Zhang, X.; Zanoni, G.; Bi, X. Silver-Catalyzed Cyclopropanation of Alkenes Using *N*-Nosylhydrazones as Diazo Surrogates. *Org. Lett.* **2017**, *19* (24), 6646−6649.
(38) Huang, Z.-D.; Ding, R.; Wang, P.; Xu, Y.-H.; Loh, T.-P. Palladium-catalyzed silylation reaction between benzylic halides and silylboronate. *Chem. Commun.* **2016**, *52* (32), 5609−5612.

https://doi.org/10.1021/acsomega.3c03519
ACS Omega 2023, 8, 38005−38012